

**DESULFURIZATION OF DIESEL FUEL BY ADSORPTION VIA  
II-COMPLEXATION USING ACTIVATED CARBON AND ALUMINA  
MODIFIED WITH Cu(I) AND Ni(II)**



Jitlada Atireklapwarodom

A Thesis Submitted in Partial Fulfilment of the Requirements  
for the Degree of Master of Science  
The Petroleum and Petrochemical College, Chulalongkorn University  
in Academic Partnership with  
The University of Michigan, The University of Oklahoma,  
Case Western Reserve University and Institut Français du Pétrole  
2010

530007

**Thesis Title:** Desulfurization of Diesel Fuel by Adsorption via  $\pi$ -Complexation Using Activated Carbon and Alumina Modified with Cu(I) and Ni(II)

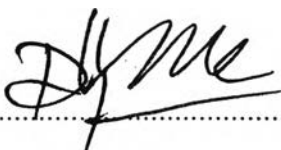
**By:** Jitlada Atireklapwarodom

**Program:** Petroleum Technology

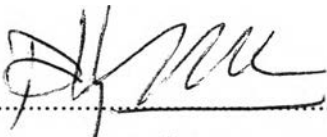
**Thesis Advisors:** Asst. Prof. Pomthong Malakul  
Dr. Michel Thomas

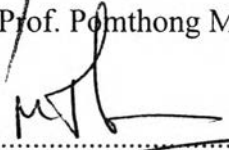
---


Accepted by the Petroleum and Petrochemical College, Chulalongkorn University, in partial fulfilment of the requirements for the Degree of Master of Science.

  
..... Dean  
(Asst. Prof. Pomthong Malakul)

**Thesis Committee:**

  
.....  
(Asst. Prof. Pomthong Malakul)

  
.....  
(Dr. Michel Thomas)

  
.....  
(Asst. Prof. Siriporn Jongpatiwut)

  
.....  
(Assoc. Prof. Metta Chareonpanich)

**ABSTRACT**

5173011063: Petroleum Technology Program

Jitlada Atireklapwarodom: Desulfurization of Diesel Fuel by Adsorption via  $\pi$ -Complexation Using Activated Carbon and Alumina Modified with Cu(I) and Ni(II).

Thesis Advisors: Asst. Prof. Pomthong Malakul and Dr. Michel Thomas 89 pp

Keywords: Adsorption/ Impregnation/ Activated carbon/ Activated alumina/ Desulfurization

The adsorptive desulfurization of simulated diesel fuel at DBT concentration of 150 ppm S was studied by using macro and mesoporous alumina (M-Al<sub>2</sub>O<sub>3</sub>, m-Al<sub>2</sub>O<sub>3</sub>) and activated carbon (AC) impregnated by Cu(II) and Ni(II), by using the incipient wetness method with an aqueous solution of CuCl<sub>2</sub> and NiCl<sub>2</sub>. Cu<sup>2+</sup> was then reduced to Cu<sup>+</sup> by H<sub>2</sub>. The effect of amount of metal loading was investigated by varying the concentration of metal at 100%, 75% and 50% of the theoretical monolayer surface coverage. The optimum adsorption temperature was found to be 30°C while the optimum flow rate was 0.4 cm<sup>3</sup>/min. The presence of metal seemed to reduce the breakthrough and adsorption capacity, the lower concentration of metal loading at 50% of the monolayer capacity for both Cu<sup>+</sup> and Ni<sup>2+</sup> on alumina showed a higher adsorption capacity than 75% and 100% probably by lowering the accessible porosity in agreement with result from B.E.T. surface area and SEM. Moreover, the smaller size at diameter 300-500  $\mu$ m which crushed after impregnation of the 100% monolayer of Cu<sup>+</sup>/m-Al<sub>2</sub>O<sub>3</sub> showed the higher breakthrough than normal size (extruded length 4 mm) and also higher than the same small size crushed before impregnation. For all among of the adsorbents, the breakthrough capacity decreased in order of 43 wt% of Cu<sup>+</sup>/AC > AC > 100% monolayer of Cu<sup>+</sup>/m-Al<sub>2</sub>O<sub>3</sub> (300-500  $\mu$ m crushed after impregnation) > non-impregnated m-Al<sub>2</sub>O<sub>3</sub> > 50% monolayer of Ni<sup>2+</sup> /m-Al<sub>2</sub>O<sub>3</sub>.

## บทคัดย่อ

จิตรลดา อติเรกลาภโรดม: การกำจัดสารประกอบกำมะถันจากน้ำมันดีเซลโดยกระบวนการดูดซับโดยใช้ถ่านกัมมันต์และอะลูมินาที่ดัดแปลงโดยคอปเปอร์และนิกเกิลเป็นตัวดูดซับ (Desulfurization of Diesel Fuel by Adsorption via  $\pi$ -Complexation Using Activated Carbon and Alumina Modified with Cu(I) and Ni(II)) อ. ที่ปรึกษา : ผศ. ดร. ปมทอง มาลากุล ณ อรุยา, ดร. มิเชล โทมัส 89 หน้า

งานวิจัยนี้ได้ศึกษากระบวนการกำจัดสารประกอบกำมะถันจากน้ำมันดีเซลโดยกระบวนการดูดซับ โดยศึกษาการดูดซับไคเบนโซไทโอฟินในแบบจำลองน้ำมันดีเซลที่มีความเข้มข้นของกำมะถันที่ 150 ส่วนต่อล้านส่วน โดยใช้ตัวดูดซับคืออะลูมินาที่มีรูพรุนขนาดใหญ่และขนาดกลาง (Macroporous และ Mesoporous alumina; M- $\text{Al}_2\text{O}_3$  และ m- $\text{Al}_2\text{O}_3$ ) และถ่านกัมมันต์ (Activated carbon หรือ AC) แล้วถูกทำให้ชุ่มด้วย  $\text{Cu}^{2+}$  และ  $\text{Ni}^{2+}$  โดยใช้สารละลายเกลือคลอไรด์ของโลหะ ( $\text{CuCl}_2$  และ  $\text{NiCl}_2$ ) ซึ่งภายหลัง  $\text{Cu}^{2+}$  จะถูกรีดิวซ์เป็น  $\text{Cu}^+$  โดยใช้ก๊าซไฮโดรเจน รวมทั้งได้มีการศึกษาอิทธิพลของปริมาณโลหะบนตัวดูดซับที่ปริมาณ 100%, 75% และ 50% ของพื้นผิวตัวดูดซับแบบชั้นเดียว (monolayer) อุณหภูมิที่เหมาะสมสำหรับการดูดซับคือ 30 องศาเซลเซียส ขณะที่อัตราการไหลที่เหมาะสมของแบบจำลองน้ำมันดีเซลคือ 0.4 ลูกบาศก์เซนติเมตรต่อนาที จากผลการทดลองพบว่า การเติมโลหะบนตัวดูดซับ ทำให้ความสามารถในการดูดซับไคเบนโซไทโอฟินลดลง โดยปริมาณ  $\text{Cu}^+$  และ  $\text{Ni}^{2+}$  ที่ 50% ของพื้นผิวตัวดูดซับ มีความสามารถในการดูดซับไคเบนโซไทโอฟินสูงกว่าที่ปริมาณ 75% และ 100% ของพื้นผิวตัวดูดซับ เนื่องจากเมื่อปริมาณโลหะเพิ่มขึ้นทำให้ความเป็นรูพรุนของตัวดูดซับลดลง ซึ่งสอดคล้องกับผลการทดลองจากการศึกษาพื้นที่ผิวด้วย B.E.T. และ SEM นอกจากนี้พบว่า 100% monolayer ของ  $\text{Cu}^+/\text{m-Al}_2\text{O}_3$  ที่เส้นผ่านศูนย์กลางของตัวดูดซับ 300-500 ไมโครเมตร ที่ถูกบดหลังจากการทำให้ชุ่มด้วย  $\text{Cu}^+$  มีความสามารถในการดูดซับมากกว่าตัวดูดซับชนิดเดียวกันที่ขนาดปกติ (ความยาว 4 มิลลิเมตร) และมากกว่าตัวดูดซับชนิดเดียวกัน ขนาดเดียวกัน ที่ถูกบดก่อนทำให้ชุ่มด้วย  $\text{Cu}^+$  และจากการศึกษาตัวดูดซับทั้งหมดพบว่า ความสามารถในการดูดซับของไคเบนโซไทโอฟินลดลงตามลำดับดังนี้ 43 wt%  $\text{Cu}^+/\text{AC}$  > AC > 100% monolayer ของ  $\text{Cu}^+/\text{m-Al}_2\text{O}_3$  (ขนาด 300-500 ไมโครเมตร ที่ถูกบดหลังจากการทำให้ชุ่มด้วย  $\text{Cu}^+$ ) > m- $\text{Al}_2\text{O}_3$  > 50% monolayer ของ  $\text{Ni}^{2+}/\text{m-Al}_2\text{O}_3$

## ACKNOWLEDGEMENTS

I would like to sincerely express my thanks and gratitude to the following people and organization. Without their help, this thesis could not be very fruitful.

First of all, I would sincerely like to thank my advisors, Asst. Prof. Pomthong Malakul and Dr. Michel Thomas, for their help and guidance on a day to day basis during my doing research at the Petroleum and Petrochemical College and IFP-Lyon. I would really appreciate their advice, suggestions, and comments.

I would like to give special thanks to Ms. Sandra Montpeyroux, Ms. Christine Bounie, Ms. Sophie Drozd, and Ms. Michèle Maricar-Pichon for their kind during my work at IFP.

I would really appreciate Asst. Prof. Siriporn Jongpatiwut and Assoc. Prof. Metta Chareonpanich, for kindly serving on my thesis committee.

I would also like to thank all my professors for their experience through their courses, giving me a chance to get knowledge about my thesis.

This thesis work is funded by the Petroleum and Petrochemical College, and by the National Center of Excellence for Petroleum, Petrochemicals, and Advanced Materials, Thailand and I would also like to express my special thank to EGIDE for financial support in France.

Thanks to all of staffs in PPC, the IFP's technicians and all the graduate students at PPC, who helped me over the year.

Thanks to all friends in Thailand and France, without their help and friendship, my beautiful experience in France can not complete.

Finally, special thanks to my family who always stand beside me in every moment, I would not have today without their support and care. Without their support this project would not have been possible. I would like to dedicate all my work to them. A million thanks would not be enough.

## TABLE OF CONTENTS

	<b>PAGE</b>
Title Page	i
Abstract (in English)	iii
Abstract (in Thai)	iv
Acknowledgements	v
Table of Contents	vi
List of Tables	ix
List of Figures	xi
<b>CHAPTER</b>	
<b>I INTRODUCTION</b>	<b>1</b>
<b>II LITERATURE REVIEW</b>	<b>3</b>
2.1 Transportation Fuels and Sulfur Specifications	3
2.1.1 Transportation Fuels	3
2.1.2 Sulfur Specification	4
2.2 Organosulfur Compounds	5
2.3 Desulfurization Process	8
2.3.1 Conventional Hydrodesulfurization (HDS)	10
2.3.2 Desulfurization by Adsorption	13
2.3.3 Adsorbents for Desulfurization	14
2.3.3.1 Activated Carbon	16
2.3.3.2 Activated Alumina	18
2.3.3.3 Molecular-Sieve Zeolite	19
2.3.3.4 Silica Gel	19
2.3.4 Previous Studies on the Use of Adsorbents for Sulfur Removal	20
2.3.5 $\pi$ -Complexation	21
2.3.6 Regeneration of Adsorbent	24

CHAPTER	PAGE
2.3.7 Fixed Bed Adsorption	25
<b>III EXPERIMENTAL</b>	27
3.1 Materials	27
3.2 Equipments	28
3.3 Methodology	28
3.3.1 Adsorbents Preparation	28
3.3.1.1 Preparation of $\text{Cu}^{2+}$ Impregnated on Activated Alumina by Using $\text{CuCl}_2$ in Deionized Water	28
3.3.1.2 Preparation of $\text{Cu}^{2+}$ Impregnated on Activated Carbon by Using $\text{CuCl}_2$ in HCl	29
3.3.1.3 Preparation of $\text{Ni}^{2+}$ Impregnated on Activated Alumina by Using $\text{NiCl}_2$ in Deionized Water	29
3.3.2 Reduction	29
3.3.3 Characterization of Adsorbents	30
3.3.4 Preparation of Simulated Diesel	30
3.3.5 Adsorption of Sulphur Compounds from Simulated Diesel by Fixed Bed Adsorption	30
3.3.6 Sulfur Concentration Analysis	32
3.3.7 Calculation Method of Breakthrough Curve	32
3.3.7.1 Definitions of the Different Volumes in the Column	34
3.3.7.2 Porosity Levels in the Column	34
3.3.7.3 First Moment of the Breakthrough Curve ( $\mu$ )	36

<b>CHAPTER</b>	<b>PAGE</b>
<b>IV RESULTS AND DISCUSSION</b>	<b>40</b>
4.1 Adsorbent Characterization	40
4.1.1 Characterization of Adsorbent by Nitrogen Adsorption/Desorption Method and Mercury Porosimetry	40
4.1.2 Temperature-Programmed Reduction of $\text{CuCl}_2$ Impregnated on the Adsorbent	47
4.1.3 Scanning Electron Microscope (SEM)	55
4.2 Fixed-Bed Adsorption Experiments	57
4.2.1 Effect of Type of Adsorbents	57
4.2.2 Effect of Feed Flow Rate	59
4.2.3 Effect of Adsorption Temperature	60
4.2.4 Effect of Amount of Metal Loading	62
4.2.5 Effect of Granulometry	71
<b>V CONCLUSIONS AND RECOMMENDATIONS</b>	<b>77</b>
5.1 Conclusions	77
5.2 Recommendations	78
<b>REFERENCES</b>	<b>79</b>
<b>APPENDICES</b>	<b>83</b>
<b>Appendix A</b> Calculation of Samples Preparation	83
<b>Appendix B</b> Calculation of Amount of Adsorption of Sulfur Compounds in Dynamic Adsorption Experiment	85
<b>CURRICULUM VITAE</b>	<b>89</b>



## LIST OF TABLES

TABLE	PAGE	
2.1	Typical compositions of transportation fuels (vol %)	3
2.2	The physical constants of the principal sulfur compounds	6
2.3	The organic sulfur compounds and their hydrotreating pathway	12
2.4	Adsorbents in commercial adsorption separations	15
2.5	Pore sizes in typical activated carbon	17
3.1	Physical properties of sulfur compounds and simulated diesel fuel	27
3.2	Gas chromatography conditions for the analysis	32
4.1	Properties of adsorbents by using the Nitrogen adsorption / desorption method at 77K	40
4.2	Properties of adsorbents by using the Mercury porosimetry	43
4.3	Reduction temperature of 100%, 75% and 50% monolayer of CuCl <sub>2</sub> impregnated on M-Al <sub>2</sub> O <sub>3</sub>	49
4.4	Reduction temperature of 100%, 75% and 50% monolayer of CuCl <sub>2</sub> impregnated on m-Al <sub>2</sub> O <sub>3</sub>	53
4.5	Hydrogen consumption of adsorbent	54
4.6	Breakthrough and adsorption capacities loading for Dibenzothiophene from simulated diesel fuel in different non-impregnated adsorbents	58
4.7	Breakthrough and adsorption capacities loading for Dibenzothiophene from simulated diesel fuel in different feed flow rate	60

<b>TABLE</b>	<b>PAGE</b>
4.8 Breakthrough and adsorption capacities loading for Dibenzothiophene from simulated diesel fuel over activated carbon at different temperature	61
4.9 Breakthrough and adsorption capacities loading for Dibenzothiophene from simulated diesel fuel over M-Al <sub>2</sub> O <sub>3</sub> at different amount of Cu <sup>+</sup> loading	63
4.10 Breakthrough and adsorption capacities loading for Dibenzothiophene from simulated diesel fuel over M-Al <sub>2</sub> O <sub>3</sub> at different amount of Ni <sup>2+</sup> loading	64
4.11 Breakthrough and adsorption capacities loading for Dibenzothiophene from simulated diesel fuel over m-Al <sub>2</sub> O <sub>3</sub> at different amount of Cu <sup>+</sup> loading	66
4.12 Breakthrough and adsorption capacities loading for Dibenzothiophene from simulated diesel fuel over m-Al <sub>2</sub> O <sub>3</sub> at different amount of Cu <sup>+</sup> loading at diameter size 300-500 μm and crushed after impregnation	67
4.13 Breakthrough and adsorption capacities loading for Dibenzothiophene from simulated diesel fuel over m-Al <sub>2</sub> O <sub>3</sub> at different amount of Ni <sup>2+</sup> loading	69
4.14 Breakthrough and adsorption capacities loading for Dibenzothiophene from simulated diesel fuel over AC and 43 wt% of Cu <sup>+</sup> loading on AC	70
4.15 Breakthrough and adsorption capacities loading for Dibenzothiophene from simulated diesel fuel over m-Al <sub>2</sub> O <sub>3</sub> at different amount of Cu <sup>+</sup> loading	72
4.16 Summarized adsorption capacity of the all adsorbent at 0.4 cm <sup>3</sup> /min and 30 °C	74
4.17 Summarized breakthrough capacity of the all adsorbent at 0.4 cm <sup>3</sup> /min and 30 °C	75

## LIST OF FIGURES

FIGURE	PAGE
2.1 The regulated sulfur levels in diesel fuel in EU, USA and Thailand.	4
2.2 Examples of sulfur compounds in petroleum.	7
2.3 GC-FPD chromatograms of gasoline, jet fuel and diesel for identification of sulfur compounds.	8
2.4 Classification of desulfurization processes based on organosulfur compound transformation.	9
2.5 Desulfurization technologies classified by nature of a key process to remove sulfur.	10
2.6 Schematic representation for desulfurization of 4,6-dimethyl-dibenzothiophene with molybdenum-based and copper(I)-based adsorbents.	22
2.7 Schematic representation for copper ions occupying faujasite 6-ring windows sites.	23
2.8 Means of interaction for a DBT molecule with NiY, corresponding to $\pi$ -complexation.	23
2.9 Idealized breakthrough curve of a fixed bed adsorber.	25
3.1 Schematic of the fixed bed adsorption breakthrough (Unit 179, IFP- Lyon, France).	31
3.2 The adsorber geometry.	32
3.3 Characteristics of a typical adsorption breakthrough curve.	36
3.4 The first moment of the breakthrough curve ( $\mu$ ).	37
4.1 Temperature-programmed reduction (TPR) of 100% monolayer $\text{CuCl}_2$ impregnated on M- $\text{Al}_2\text{O}_3$ in 10% $\text{H}_2$ in Ar.	47
4.2 Temperature-programmed reduction (TPR) of 75% monolayer of $\text{CuCl}_2$ impregnated on M- $\text{Al}_2\text{O}_3$ in 10% $\text{H}_2$ in Ar.	48

<b>FIGURE</b>	<b>PAGE</b>
4.3 Temperature-programmed reduction (TPR) of 50% monolayer of CuCl <sub>2</sub> impregnated on M-Al <sub>2</sub> O <sub>3</sub> in 10% H <sub>2</sub> in Ar.	48
4.4 Summary curve of temperature-programmed reduction (TPR) of 100%, 75% and 50% monolayer of CuCl <sub>2</sub> impregnated on M-Al <sub>2</sub> O <sub>3</sub> in 10% H <sub>2</sub> in Ar.	49
4.5 Temperature-programmed reduction (TPR) of 100% monolayer of CuCl <sub>2</sub> impregnated on m-Al <sub>2</sub> O <sub>3</sub> in 10% H <sub>2</sub> in Ar.	51
4.6 Temperature-programmed reduction (TPR) of 75% monolayer of CuCl <sub>2</sub> impregnated m-Al <sub>2</sub> O <sub>3</sub> in 10% H <sub>2</sub> in Ar.	51
4.7 Temperature-programmed reduction (TPR) of 50% monolayer of CuCl <sub>2</sub> impregnated on m-Al <sub>2</sub> O <sub>3</sub> in 10% H <sub>2</sub> in Ar.	52
4.8 Summary curve of temperature-programmed reduction (TPR) of 100%, 75% and 50% monolayer of CuCl <sub>2</sub> impregnated on m-Al <sub>2</sub> O <sub>3</sub> in 10% H <sub>2</sub> in Ar.	52
4.9 SEM images of surface and cross-section of adsorbents (CuCl <sub>2</sub> impregnated on M-Al <sub>2</sub> O <sub>3</sub> and m-Al <sub>2</sub> O <sub>3</sub> ).	56
4.10 SEM images of surface and cross-section of small particle of 100% monolayer CuCl <sub>2</sub> / m-Al <sub>2</sub> O <sub>3</sub> crushed before impregnation at diameter size 300-500 μm.	57
4.11 Breakthrough curve at of Dibenzothiophene in a fixed-bed adsorber at 0.4 cm <sup>3</sup> /min and 30 °C over M-Al <sub>2</sub> O <sub>3</sub> , m-Al <sub>2</sub> O <sub>3</sub> and AC.	58
4.12 Breakthrough curve at of Dibenzothiophene in a fixed-bed adsorber at 30 °C over m-Al <sub>2</sub> O <sub>3</sub> at feed flow rate 2 cm <sup>3</sup> /min and 0.4 cm <sup>3</sup> /min.	59
4.13 Breakthrough curve of Dibenzothiophene in a fixed-bed adsorber over m-Al <sub>2</sub> O <sub>3</sub> at 0.4 cm <sup>3</sup> /min by varying temperature at 30 °C and 90 °C.	61

FIGURE	PAGE
4.14 Breakthrough curve of Dibenzothiophene in a fixed-bed adsorber at 0.4 cm <sup>3</sup> /min and 30 °C over M-Al <sub>2</sub> O <sub>3</sub> , 100% monolayer Cu <sup>+</sup> /M-Al <sub>2</sub> O <sub>3</sub> , 75% monolayer Cu <sup>+</sup> /M-Al <sub>2</sub> O <sub>3</sub> and 50% monolayer Cu <sup>+</sup> /M-Al <sub>2</sub> O <sub>3</sub> .	62
4.15 Breakthrough curve of Dibenzothiophene in a fixed-bed adsorber at 0.4 cm <sup>3</sup> /min and 30 °C over M-Al <sub>2</sub> O <sub>3</sub> , 100% monolayer of Ni <sup>2+</sup> /M-Al <sub>2</sub> O <sub>3</sub> , 75% monolayer of Ni <sup>2+</sup> /M-Al <sub>2</sub> O <sub>3</sub> and 50% monolayer of Ni <sup>2+</sup> /M-Al <sub>2</sub> O <sub>3</sub> .	64
4.16 Breakthrough curve of Dibenzothiophene in a fixed-bed adsorber at 0.4 cm <sup>3</sup> /min and 30 °C over m-Al <sub>2</sub> O <sub>3</sub> , 100% monolayer of Cu <sup>+</sup> /m-Al <sub>2</sub> O <sub>3</sub> , 75% monolayer of Cu <sup>+</sup> /m-Al <sub>2</sub> O <sub>3</sub> and 50% monolayer of Cu <sup>+</sup> /m-Al <sub>2</sub> O <sub>3</sub> .	65
4.17 Breakthrough curve of Dibenzothiophene in a fixed-bed adsorber at 0.4 cm <sup>3</sup> /min and 30 °C over m-Al <sub>2</sub> O <sub>3</sub> crushed after impregnation at diameter size 300-500 μm, m-Al <sub>2</sub> O <sub>3</sub> , 100% monolayer of Cu <sup>+</sup> /m-Al <sub>2</sub> O <sub>3</sub> , 75% monolayer of Cu <sup>+</sup> /m-Al <sub>2</sub> O <sub>3</sub> and 50% monolayer of Cu <sup>+</sup> /m-Al <sub>2</sub> O <sub>3</sub> .	67
4.18 Breakthrough curve of Dibenzothiophene in a fixed-bed adsorber at 0.4 cm <sup>3</sup> /min and 30 °C over m-Al <sub>2</sub> O <sub>3</sub> , 100% monolayer of Ni <sup>2+</sup> /m-Al <sub>2</sub> O <sub>3</sub> , 75% monolayer of Ni <sup>2+</sup> /m-Al <sub>2</sub> O <sub>3</sub> and 50% monolayer of Ni <sup>2+</sup> /m-Al <sub>2</sub> O <sub>3</sub> .	68
4.19 Breakthrough curve of Dibenzothiophene in a fixed-bed adsorber at 0.4 cm <sup>3</sup> /min and 30 °C over AC and 43% wt of Cu <sup>+</sup> /AC.	70

FIGURE	PAGE
4.20 Breakthrough curve of Dibenzothiophene in a fixed-bed adsorber at 0.4 cm <sup>3</sup> /min and 30 °C over different size and preparation of 100% monolayer of Cu <sup>+</sup> /m-Al <sub>2</sub> O <sub>3</sub> ; extruded length 4 mm, crushed before impregnation at diameter size 300-500 μm and crushed after impregnation at diameter size 300-500 μm.	71
4.21 Summary graph of adsorption capacity of the all adsorbent in order of highest to lowest adsorption capacity at 0.4 cm <sup>3</sup> /min and 30 °C.	73
4.22 Summary graph of breakthrough capacity of the all adsorbent in order of highest to lowest adsorption capacity at 0.4 cm <sup>3</sup> /min and 30 °C.	73
B1 Breakthrough curve without adsorbent.	85